Available online at www.sciencedirect.com
SCIENCE DIRECT®
Catalysis Today 89 (2004) 343–355
CATALYSIS TODAY
www.elsevier.com/locate/cattod

First principles study of structural, electronic, elastic and optical properties of MgS, MgSe and MgTe

F. Drief, A. Tadjer*, D. Mesri, H. Aourag

CMSL, Département de Physique, Faculté de Sciences, Université de Sidi-Bel-Abbes, BP 89, Route de Tlemcen, Sidi-Bel-Abbes 22000, Algeria

Abstract

We report first principles calculations of structural, electronic, elastic and optical properties of Mg-based compounds in zinc blende and rocksalt structures employing the density functional theory (DFT) within the local density approximation (LDA) using the full potential linearised augmented plane wave (FPLAPW) method. Results include lattice parameters, band structure, total and partial density of states, charge density and optical properties of MgS, MgSe and MgTe semiconductors in zinc blende and rocksalt structures.

Keywords: First principles calculations; Electronic and structural properties; MgX compounds

1. Introduction

Wide band gap semiconductors are attracting an enormous technological interest both because of their potential use in devices capable of operating at high power level and high temperature and because of need for optical materials active in blue-green spectral range.

Complex quantum structures such as quantum wells and wires, self organised quantum dots, laser structures and microcavities are grown using either II–VI materials (CdTe, ZnTe and MgTe).

It is well known that II–VI semiconductors have a large optical gaps, but only recently the feasibility of green-blue opto-electronic devices based on these materials has been demonstrated.

Unlike ZnSe and ZnTe which have been extensively studied, very little about MgS, MgSe and MgTe.

Compared Mg (belongs to column IIA in the periodic table)-based semiconductors column IIB compounds, such as ZnSe and ZnTe, are very different in the electronic and bonding properties. This difference was attributed to the existence of a metal d band inside the main valence band in column IIB compounds semiconductors. The absence of d orbital in group IIA elements results in lowering the valence band maximum and widening the band gap; thus, the superlattices made of ZnMg-VI and Zn-VI compounds were suggested to be type-I superlattices [1].

The imperfect d orbital screening in the group IIB elements is relatively tightly bonded, and this bond property leads to the tetrahedrally bonded structures, such as zinc blende and wurtsite, while the rocksalt structure is more favourable for group IIA elements.

In this paper, we examine the structural, electronic and optical properties of MgS and MgSe and MgTe using full potential linearised augmented plane wave (FPLAPW) method in zinc blende and rocksalt structures within a local density approximation (LDA) applying the code WIEN'97.

The rest of the paper is organised as follows: in Section 2 we describe briefly the method to be used, Section 3 contains our results and discussion and finally in Section 4 we summarise our conclusions.

2. Method of calculation

The full potential linearised augmented plane wave method [2] is among the most accurate methods for performing electronic structure calculations for crystals. It is based on the density functional theory [4] in the usual Kohn and Sham approach [3] for the treatment of exchange and correlation, and use the local spin density approximation (LSDA) [5,6]. The FPLAPW method is a procedure for solving the Kohn and Sham equations for the ground-state density, total energy and Kohn and Sham eigenvalues

* Corresponding author. Tel.: +213-4854-1928; fax: +213-4854-1152.
E-mail address: aek.tadjer@eudoramail.com (A. Tadjer).

0920-5861/$ – see front matter © 2003 Elsevier B.V. All rights reserved.
doi:10.1016/j.cattod.2003.12.013

(energy bands) of a many electron system by introducing a basic set which is especially adapted to the problem. The FPLAPW method divides space into an interstitial region (IR) and non-overlapping (MT) spheres centred at the atomic sites. In the IR, the basis set consists of plane waves. Inside the MT spheres, the basis set is described by radical solutions of the one particle Schrodinger equation (at fixed energy) and their energy derivatives multiplied by spherical harmonics.

In order to achieve energy eingenvalues convergence, we have expanded the basis function up to $R_{max} = 8$ (where K_{max} is the maximum modulus for the reciprocal lattice vector and RMT is the average radius of the MT spheres). Furthermore, we adopted the values of 2.0 bohr for Mg, 2.2 bohr for S, 2.2 bohr for Se and 2.6 bohr for Te as MT radii. The K integration over the Brillouin zone is performed up to a $4 \times 4 \times 4$ Monkhost and Pack [7] mesh (20 points in the irreducible wedge of the Brillouin zone are used in rocksalt and zinc blende structures for MgS, MgSe and MgTe). The iteration process was repeated until the calculated total energy of the crystal converged to less than 1 mRy.

3. Results and discussion

3.1. Structural properties

Within DFT LSDA calculations the structural properties (crystal structure, equilibrium lattice constant, bulk modulus) are very important first step toward understanding the material properties from microscopic view point.

The calculated ground-state energies are plotted as a function of the lattice constants for Mg^{-} compounds in two structures: zinc blende and rocksalt (see Fig. 1). The common procedure for the determination of the structural properties near equilibrium consists in computing the total energy at different values of the lattice parameter and in fitting the results to a semiempirical equation of states. In this work we use the Murnaghan equation of states [8].

In agreement with experiment, at zero pressure, the rocksalt phase is found most stable for the Mg chalcogenides as shown in Fig. 1. The preference of these phase over the zinc blende structure is consistent with the picture that materials with higher f_i values favour more ionic structures like rocksalt.

In Table 1, we present our calculated bulk modulus (B), first derivative of B (B') and equilibrium lattice constant (a), compared to experimental and theoretical values. The theoretical predictions agree within 1% with experimental results for MgS and MgSe and within 2% for MgTe, an accuracy typical of LDA calculations. The structural parameters, of MgS and MgSe in both structures, are underestimated because LDA uses, but the lattice parameters of MgTe compound are, quite unusually, overestimated in both structures.

We remark that the bulk modulus is overestimated with 6% for MgS and MgSe in both phases, zinc blende and rocksalt; for MgTe we have found 2% in zinc blende structure and rocksalt structure compared with theoretical results [9,11].

We remark that a value of bulk modulus for MgS in zinc blende structure is a same compared with the result in Ref. [10].

We note however that for the latter materials experimental data are not directly measured in zinc blende phase, but extrapolated from the ternary alloys, the pure materials being unstable in that phase. A few ab initio theoretical results for zinc blende MgSe show different equilibrium lattice constants, $a_0 = 5.87$–6.07 Å, and our result falls in this region.

3.2. Electronic properties

3.2.1. Electronic band structures

In the following calculation, we have distinguished the Mg ($1s^2\ 2s^2$), S ($1s^2\ 2s^2\ 2p^6$), Se ($1s^2\ 2s^2\ 2p^6\ 3s^2\ 3p^6$) and Te ($1s^2\ 2s^2\ 2p^6\ 3s^2\ 3p^6\ 3d^{10}\ 4s^2\ 4p^6$) inner-shell electrons from the valence band electrons of the Mg ($2p^6\ 3s^2$), S ($3s^2\ 3p^4$), Se ($3d^{10}\ 4s^2\ 4p^4$) and Te ($4d^{10}\ 5s^2\ 5p^4$) shells.

The band structure of the constituents (MgS, MgSe and MgTe) in two phases (zinc blende and rocksalt) have been calculated at theoretical equilibrium lattice constant rather than at the experimental one. This choice appears to be more consistent with the structural calculations, and the comparison with experimental data yields better results both qualitatively and quantitatively (see Figs. 2 and 3).

For MgS the valence band maximum and the conduction band minimum occur at Γ for zinc blende structure, and valence band maximum occur at Γ and the conduction band minimum occur at X point for rocksalt structure. The same trend was found in MgSe and MgTe. So, these materials are predicted to have direct band gap in zinc blende structure for MgS, MgSe and MgTe, and indirect band gap in X for rocksalt structure.

DFT-derived fundamental band gaps are, as usual, underestimated, but a precise determination of the error is not possible, as previously discussed for the Mg chalcogenides.

In Table 2, we summarised the calculated gap energetic for MgS, MgSe and MgTe in rocksalt and zinc blende structure. We compare our results with experimental data extrapolated from the ternary alloys in zinc blende structure, and we remark that the obtained results are underestimated with 30%. This underestimation is due to LDA use.

3.2.2. Total and partial density of states

In this section, we present the calculated total and partial DOS of MgS, MgSe and MgTe in zinc blende and rocksalt structures. We also analyse the DOS at the atoms (anion (S, Se or Te) and cation (Mg)). The DOS was computed using (2 8 5) and (1 6 5) k points in the irreducible Brillouin zone for zinc blende and rocksalt structures, respectively.

Figs. 4 and 5 show the total and the projected DOS integrated over the atom spheres for MgS, MgSe and MgTe in zinc blende and rocksalt structures. These plots (figure) are very similar for both rocksalt and zinc blende structures

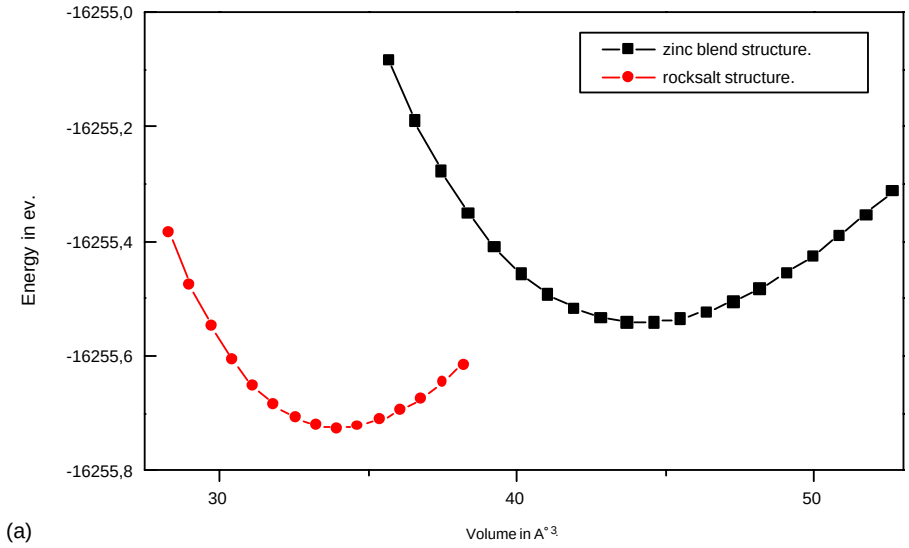

(a)

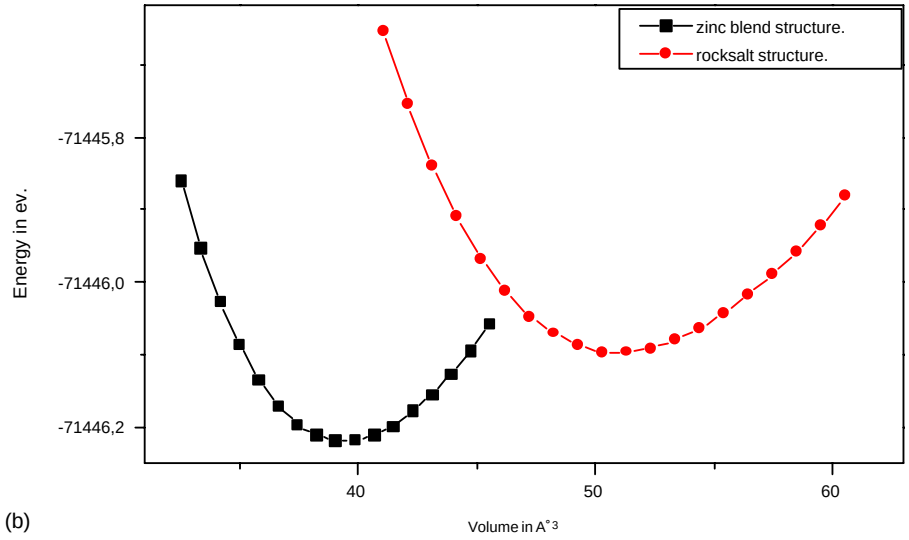

(b)

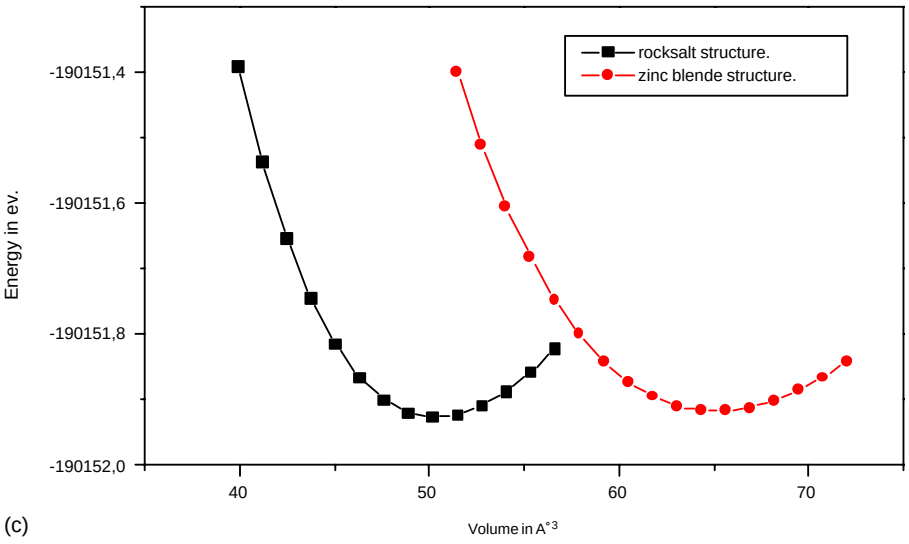

(c)

Fig. 1. Total energy E vs. volume V for rocksalt and zinc blende structure for MgS, MgSe and MgTe.

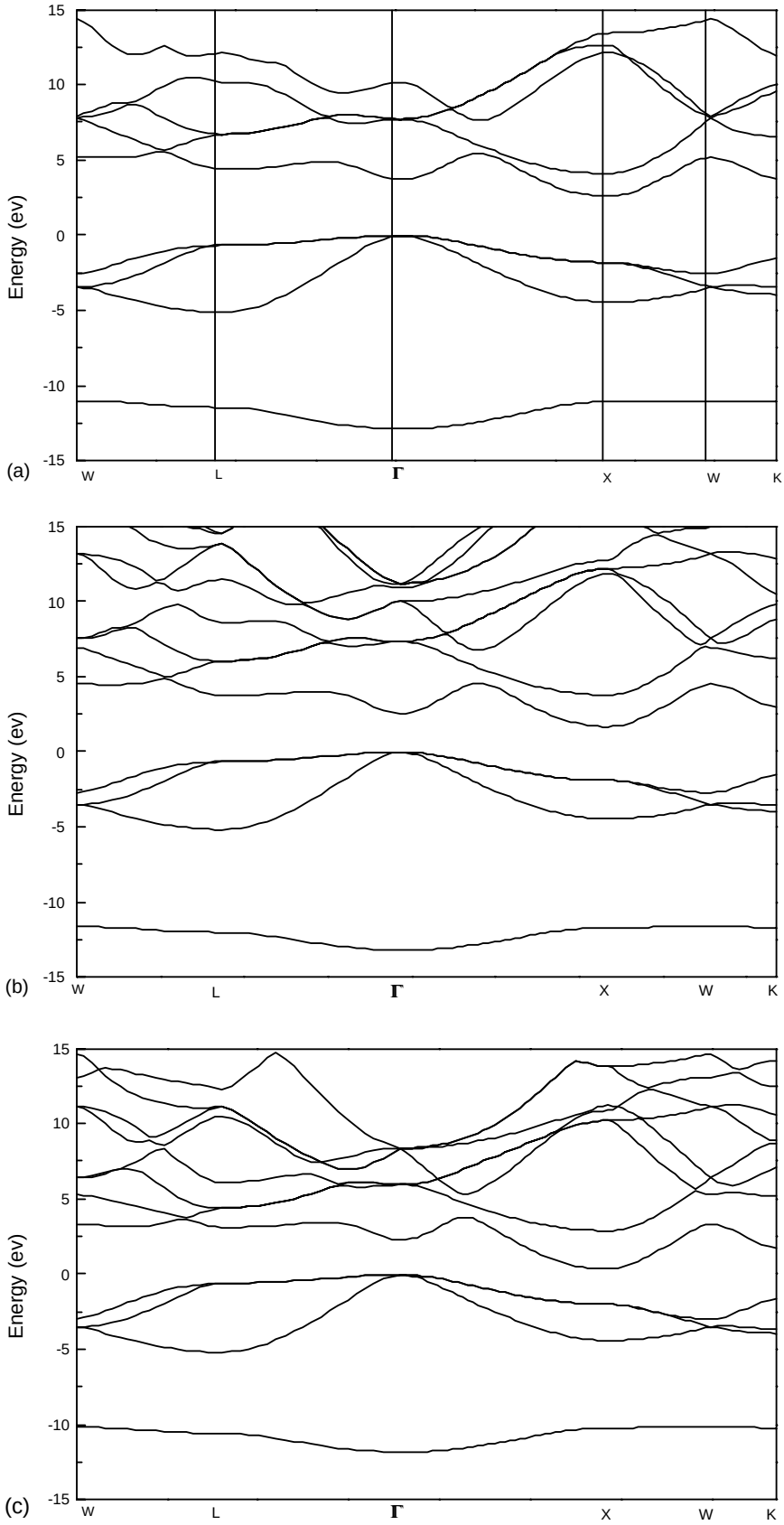

Fig. 2. LDA band structure of (a) MgS, (b) MgSe and (c) MgTe in rocksalt structure along the principal high-symmetry directions in the Brillouin zone.

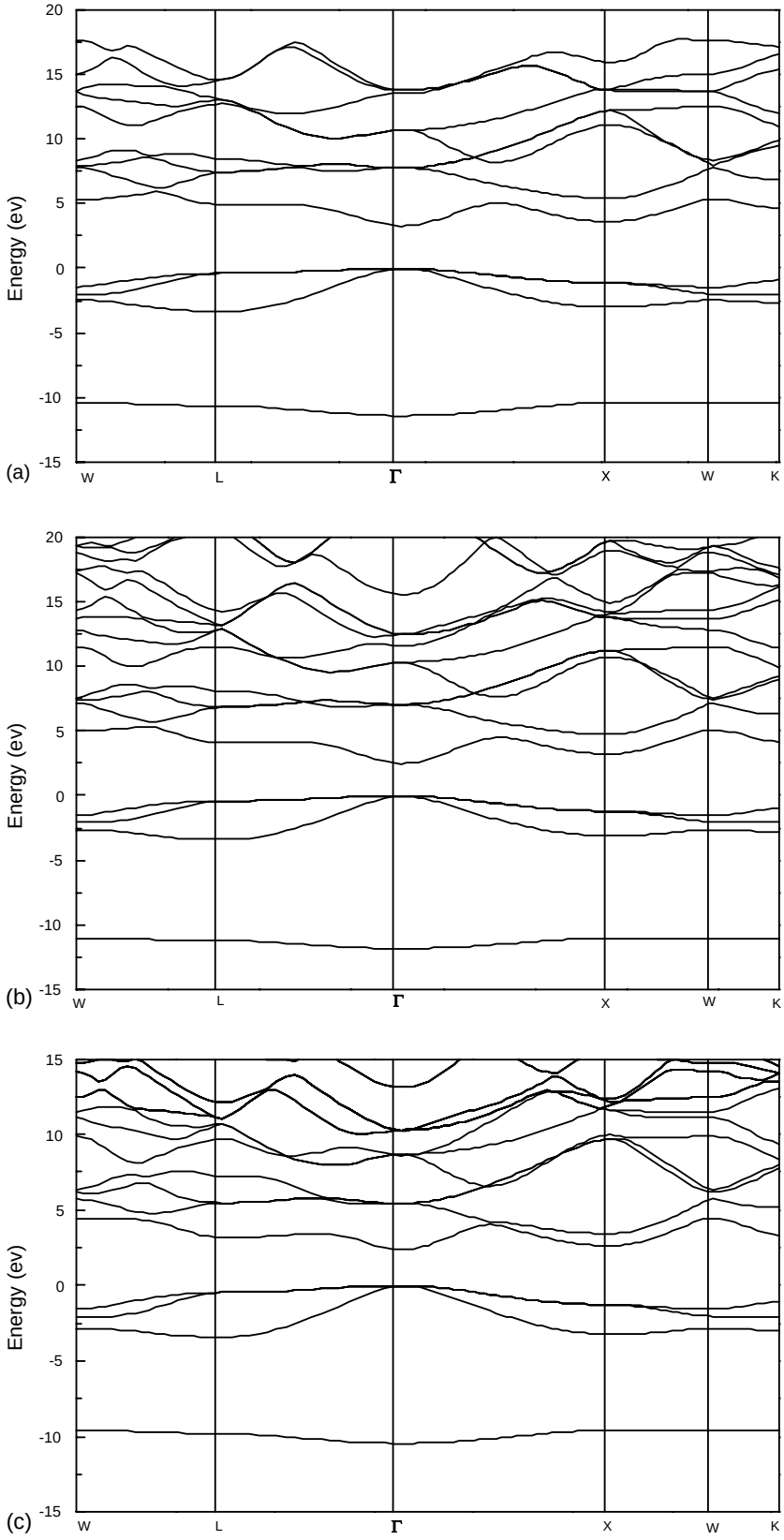

Fig. 3. LDA band structure of (a) MgS, (b) MgSe and (c) MgTe in zinc blende structure along the principal high-symmetry directions in the Brillouin zone.

Table 1
Structure parameters of MgS, MgSe and MgTe in zinc blende and rocksalt structure calculated in equilibrium parameter and compared with theoretical and experimental data

Compound	Zinc blende			Rocksalt		
	Calculated	Theoretical	Experimental	Calculated	Theoretical	Experimental
MgS						
a (Å)	5.612	5.584 [9] 5.615 [10] 5.622 [17]	5.619 [19]	5.142	5.135 [9]	5.203
B (kbar)	612	575 [9] 612 [10]		828	777 [9]	
B'	4.06	3.7 [9]		3.98	3.5 [9]	
MgSe						
a (Å)	5.886	5.873 [9]	5.89 [19]	5.401	5.406 [9]	5.451
B (kbar)	505	470 [9]		683	627 [9]	
B'	4.02	3.7 [9]		4.15	3.5 [9]	
MgTe						
a (Å)	6.38	6.36 [11] 6.37 [16]	6.36 [18]	5.86	5.84 [11] 5.85 [16]	
B (kbar)	387	376 [11]		520	533 [11]	
B'	3.89			4.1		

(MgS, MgSe and MgTe). While not much difference is expected between DOSs obtained for the two structures for occupied states (valence bands), significant discrepancies are obvious for the unoccupied levels (conduction bands).

For both structures of MgS, MgSe and MgTe the total DOS presents three regions: the lower part of the valence bands is dominated by S 3s, Se 4s and Te 5s states in MgS, MgSe and MgTe, respectively, and upper part by S 3p, Se 4p and Te 5p states in MgS, MgSe and MgTe, respectively. The Mg 3p and Mg 3s states contribute in the upper part of the valence bands. The first conduction band in Γ is predominantly of Mg 3s and Mg 3p states.

3.2.3. Total valence charge densities and ionicity factor

To visualise the nature of the bond character and to explain the charge transfer and bonding properties of our compounds, we calculate the total charge density. The calculated electron charge distributions indicate that there is a strong ionic character for both structures as can be seen along the Mg–S, Mg–Se and Mg–Te bonds. The S, Se and Te ions are larger than the Mg ions for both cases in Figs. 6 and 7. Besides, one notice that the situation in zinc blende structure is analogous to that of the rocksalt structure. A plot of the charge densities in Figs. 6 and 7 clearly shows a net charge transfer from Mg to S, Mg to Se and Mg to Te of the MgS, MgSe and MgTe, respectively, because the S, Se and Te are more electronegative than Mg.

The case of ionicity is interesting since it can be related to properties of the charge density on the whole and features in the band structure. The ionicity which is directly associated to the character of the chemical bond provides us a means for explaining and classifying the properties of these II–VI compounds. It is well known that the ionicity character is highly dependent on the total valence charge densities by calculating the charge distribution. The calculated ionicity values for MgS, MgSe and MgTe compared with those of Phyllips [12], and Garcia and Cohen [13] are summarised in Table 3.

Our results indicate that MgS, MgSe and MgTe exhibit large ionicity character, which indicates that Mg compounds are the more ionic materials in II–VI family.

Table 2
The gap energetic calculated for MgS, MgSe and MgTe in rocksalt and zinc blende structures

Compound	E_g^{zinc} (eV)	Experimental value (eV)	E_g^{rock} (eV)
MgS	3.371 (this work)	4.5 [21]	2.208 (this work)
MgSe	2.825 (this work)	3.6 [22] 2.47 [20]	1.952 (this work)
MgTe	2.615 (this work)	3.47 [23] 2.29 [20]	0.414 (this work)

3.3. Elastic properties

The full potential linearised augmented plane waves method allows total energy calculations to be done for arbitrary crystal structures. We can therefore apply small strains to the equilibrium lattice, determine the resulting change in the total energy, and from this information deduce the

Table 3
The ionicity calculated with Garcia and Cohen method for MgS, MgSe and MgTe in rocksalt and zinc blende structures

Compound	f_i^{zinc} (eV)	f_i^{rock} (eV)	Experimental value
MgS	0.639[a]	0.779[a]	0.786 [12]
MgSe	0.619[a]	0.727[a]	0.790 [12]
MgTe	0.525[a]	0.720[a]	0.554 [12]

[a] Calculated using the Garcia and Cohen approach [13].

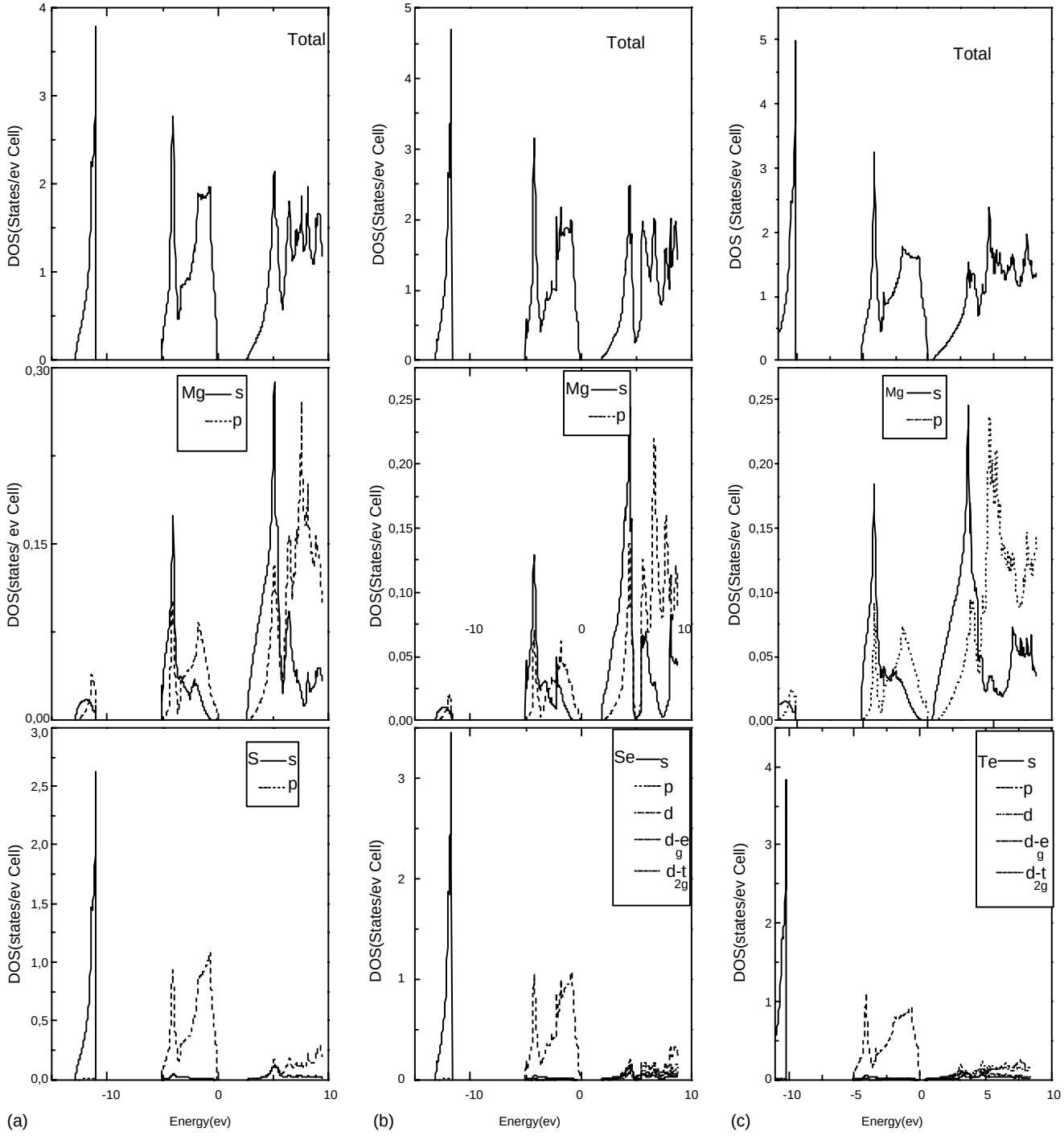

Fig. 4. Calculated total and partial density of states in rocksalt structure of (a) MgS, (b) MgSe and (c) MgTe.

elastic modulo. The calculation of the modulo allows us garner information about non-equilibrium properties from our simple initial system. So the calculated elastic constants can then be used to check the experimental bulk and shear modulo, if available.

3.3.1. Theoretical background and notations

Let E^0_{tot} be the total energy of an initial crystal and V_0 its volume. By bending this crystal, the energy of the resulting strained state can be expressed as

$$E_{\text{tot}} = E^0_{\text{tot}} + P(V - V_0) + \phi_{\text{elast}}$$

where V is the volume of the strained lattice, ϕ_{elast} the elastic energy, and P the pressure defined by

$$P = -\left(\frac{\partial E_{\text{tot}}}{\partial V}\right) V_0$$

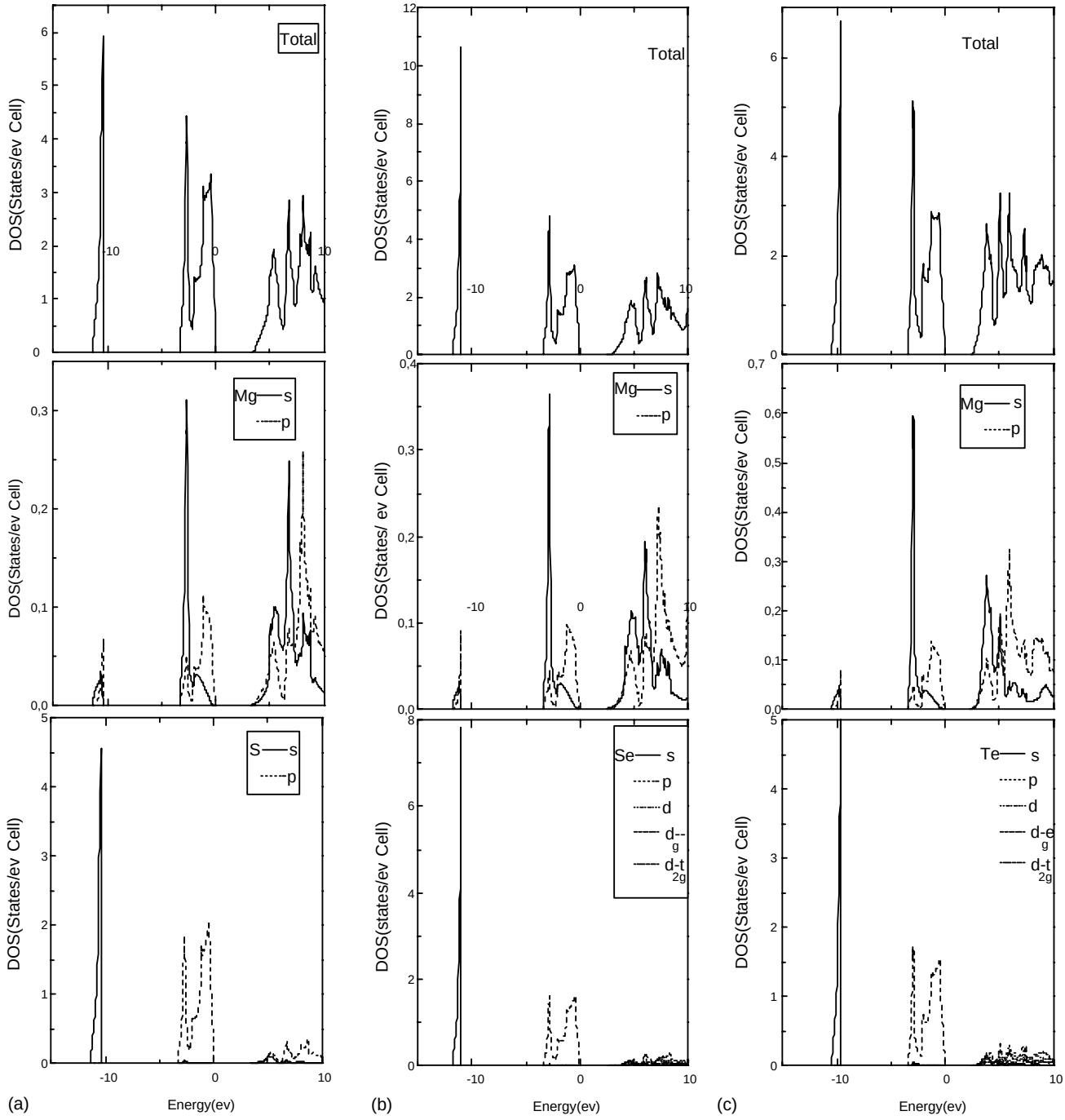

Fig. 5. Calculated total and partial density of states in zinc blende structure of (a) MgS, (b) MgSe and (c) MgTe.

To first order, the strained lattice (lattice vectors $\vec{a}$) is related to the unstriated lattice ($\vec{a}_{\mathrm{D}}$) by

$$\vec{a} = (I + \xi)\vec{a}_{\mathrm{D}}$$

where I is the identity matrix and ξ the strain tensor. According to Hooke's law, the linear elastic constants C_{ijkl} are then defined by using the second-order development of the elastic energy in Voigt's two-suffix notation:

$$\phi_{\mathrm{elast}} = \tfrac{1}{2} V C_{ij} \xi_{ij}, \quad i, j = 1\text{–}6$$

Thus, it is possible to derive elastic constants from the second-order derivatives of E_{tot}:

$$C_{ij} = \frac{1}{V_0} \frac{\partial^2 E_{\mathrm{tot}}}{\partial \xi_i \partial \xi_j}$$

A cubic crystal has only three independent constants, C_{11}, C_{12}, and C_{44}, leading to an effective elastic tensor.

The calculated elastic constants for MgS, MgSe and MgTe in zinc blende and rocksalt structure are given in Table 4. Unfortunately, there are no experimental elastic constants

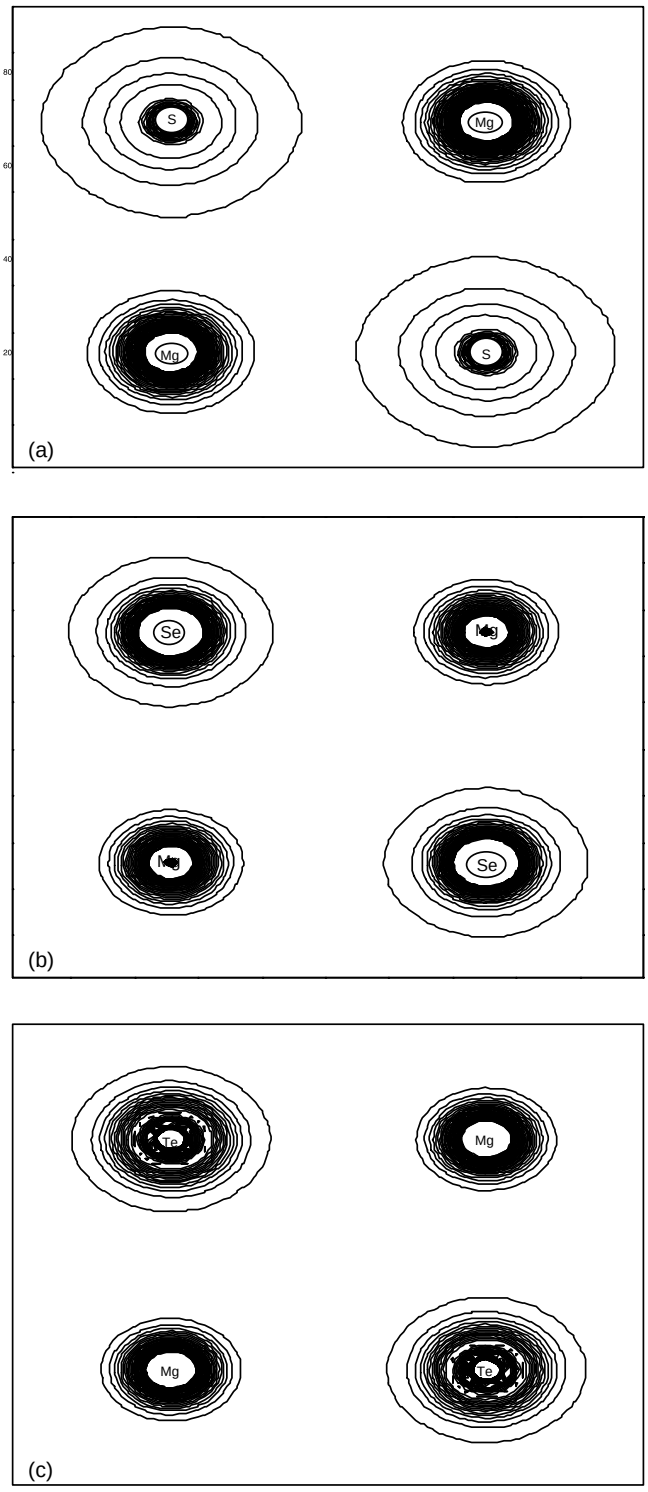

Fig. 6. Contour plots of the total valence densities in (1 0 0) plane of (a) MgS, (b) MgSe and (c) MgTe in rocksalt structure.

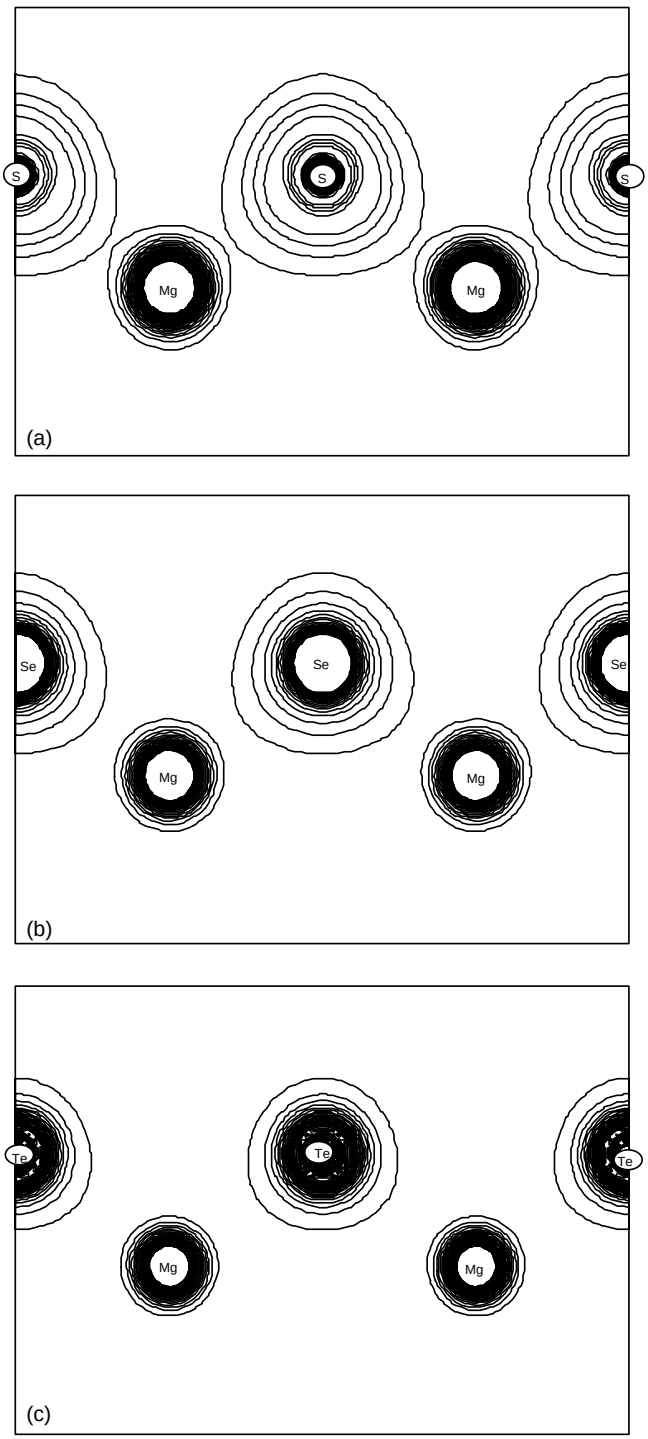

Fig. 7. Contour plots of the total valence densities in (1 1 0) plane of (a) MgS, (b) MgSe and (c) MgTe in zinc blende structure.

available since a suitable single crystal of MgS and MgSe has not been obtained so far. We have compared our elastic constant results for MgS in zinc blende structure with theoretical data [10] and we remark that they are in good agreement.

3.4. Optical properties

Optical properties are of fundamental importance, since these involve not only the occupied and unoccupied parts of the electronic structure, but also carry information on the character of the bands. In order to elucidate the anisotropy in the optical properties of MgS, MgSe and

Table 4
Elastic constants calculated for MgS, MgSe and MgTe in zinc blende and rocksalt structure in unit of GPa

Compound	Zinc blende				Rocksalt		
	C_{11}	C_{12}	C_{44}	$2C_{12}/C_{11}$	C_{11}	C_{12}	C_{44}
MgS	72.37 (74.00 [10]; 56.80 [24])	55.76 (54.70 [10]; 57.90 [24])	58.41		183.45	34.92	69.01
MgSe	63.22	43.86	44.76		209.07	31.32	74.37
MgTe	61.24	28.17	48.27	0.92 (1.06 [25])	82.81	25.73	38.96

MgTe the calculated dielectric function is a very important step.

3.4.1. The dielectric function

Optical properties of matter can be described by means of the transverse dielectric function $\xi(q,\omega)$ where q is the momentum transfer in the photon–electron in traction and ω the energy transfer. The real and imaginary parts of $\xi(\omega)$ are often referred to as $\xi_1(\omega)$ and $\xi_2(\omega)$, respectively ($\xi(\omega) = \xi_1(\omega) + \xi_2(\omega)$). In the condensed matter systems, there are two contributions to $\xi(\omega)$, viz. intraband and interband transitions. The contribution from intraband transitions is important only for metals. The interband transitions can further be split into direct and indirect transitions.

3.4.1.1. The imaginary part. The direct interband contribution to the imaginary part of the dielectric function $\xi_2(\omega)$ is calculated by summing all possible transitions from occupied to unoccupied states, taking the appropriate transition matrix element into account. The interband contribution to the diagonal element of $\xi_2(\omega)$ is given by

$$\xi_2(\omega) = \frac{8\pi^2 e^2}{m^2\omega^2} \sum_{n}^{\text{unocc}} \sum_{n'}^{\text{occ}} \int_{\text{BZ}} |P^{v}_{nn'}(k)|^2 f_{kn}(1 - f_{kn'}) \partial(E^k_n(k) - E^k_{n'} - \hbar\omega) \frac{\partial^3 k}{(2\pi)^3}$$

where e is the electron charge, m its mass, f_{kn} the Fermi–Dirac function distribution, $P^{v}_{nn'}$ the projection of the momentum matrix elements along the direction v of the electric field and E^k_n the one-electron energy. The evaluation of the matrix elements is done separately over the MT and interstitial regions. Further details about the evaluation of matrix elements are found in Ref. [14].

We have performed this calculations using 47 and 60 irreducible k points for the Brillouin zone for MgS, MgSe and MgTe in the rocksalt and zinc blende structure, respectively.

We first look at the rocksalt phase of MgS. The main peaks, as seen in Fig. 8(a), are 6.04, 7.49, 8.22 eV. For the first two peaks, the strongly contributing regions of k space are much the same as for the III–V materials [15]. We find that 6.04 eV peak is primarily due to transitions in Γ to L region; the 7.49 eV peak is associated with transitions in the Γ to X and X to U regions. The last peak at 8.22 eV does not seem to be due to transitions in Γ to L region as in III–V materials, but rather from Γ to X and X to U regions.

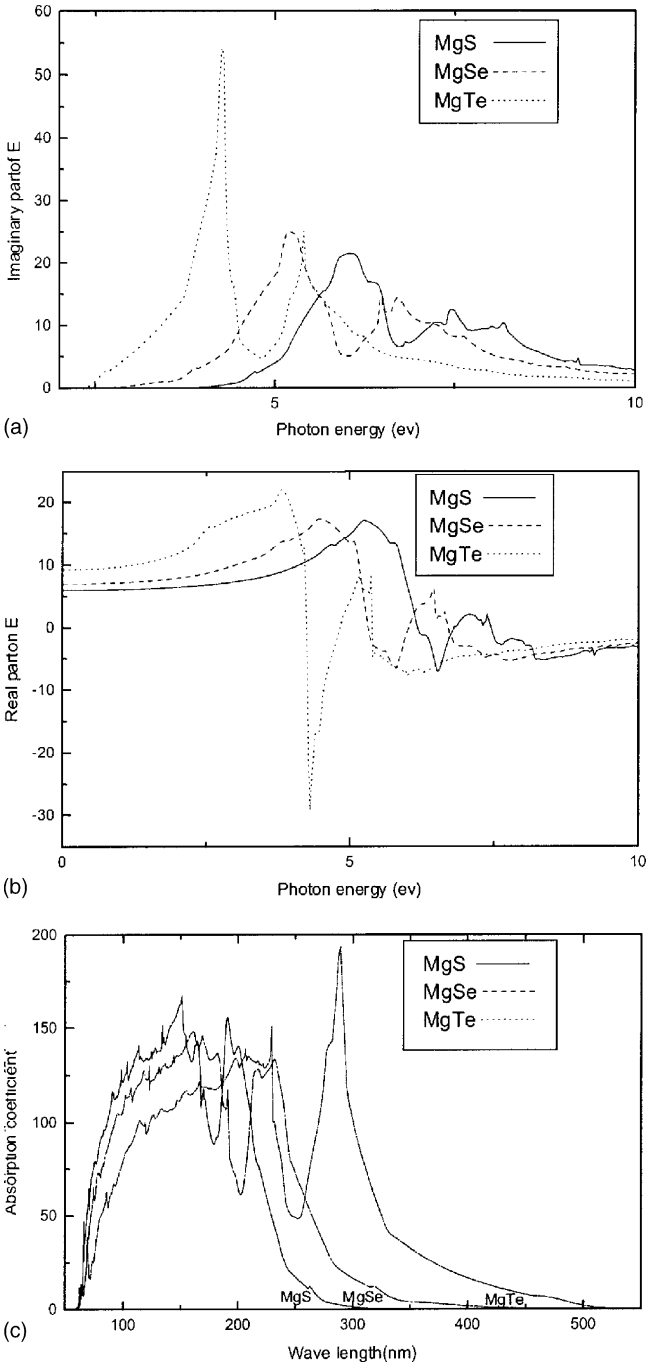

Fig. 8. (a) Imaginary and (b) real parts of dielectric function and (c) absorption coefficient of MgS, MgSe and MgTe in rocksalt structure.

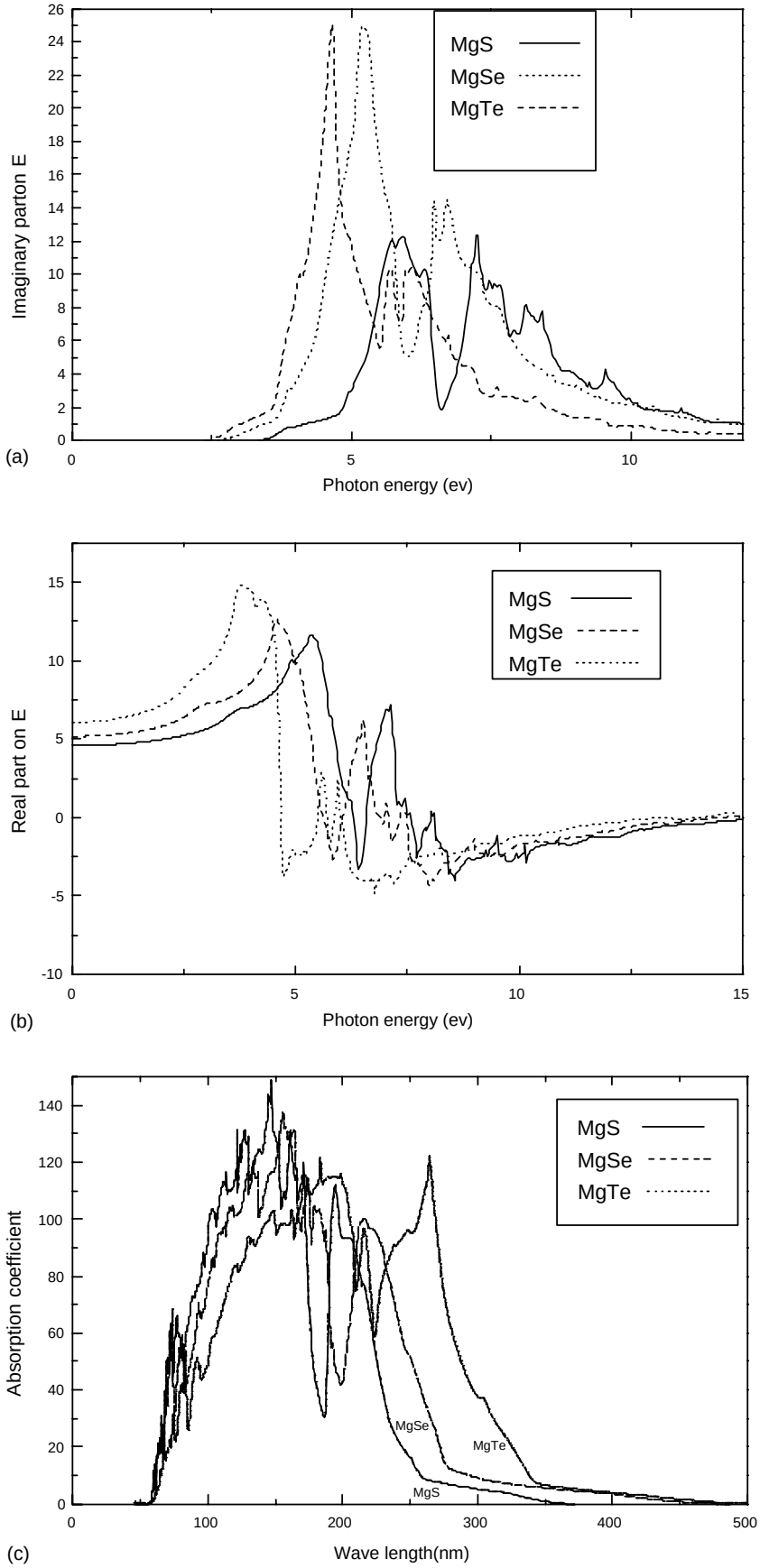

Fig. 9. (a) Imaginary and (b) real parts of dielectric function and (c) absorption coefficient of MgS, MgSe and MgTe in zinc blende structure.

For MgSe in the rocksalt structure the main peaks, as seen in Fig. 8(a), are 5.21, 6.51 and 6.76 eV. We find that 5.21 eV peak is primarily due to transitions in Γ to L region; the 6.51 eV peak is associated with transitions in Γ to X and X to U regions. The last peak at 6.76 eV is due to transitions in Γ to X and X to U regions. For MgTe in rocksalt structure we remark that two peaks, as seen in Fig. 8(a), are 4.32 and 5.46 eV due to Γ to L and Γ to X regions, respectively.

The same results are remarked for MgS, MgSe and MgTe in zinc blende structure. The main peaks, as seen in Fig. 9(a), are 5.90, 7.25 and 8.12 eV for MgS, 5.20, 6.49 and 6.73 eV for MgSe and 4.65, 5.71 and 6.09 eV for MgTe. We find that first peak (5.90 eV for MgS, 5.20 eV for MgSe and 4.65 eV for MgTe) is primarily due to transitions in Γ to L region; the second peak (7.25 eV for MgS, 6.49 eV for MgSe and 5.71 eV for MgTe) is associated with transitions in the Γ to X and X to U regions. The last peak at (8.12 eV for MgS, 6.73 eV for MgSe and 6.09 eV for MgTe) does not seem to be due to transitions in Γ to L region as in III–V materials, but rather due to transitions in Γ to X and X to U regions.

3.4.1.2. The real part (static dielectric function). The real part of the frequency-dependent response functions, $\xi_1(\omega)$, has been obtained from imaginary part, $\xi_2(\omega)$, by using the Kramers–Kronig transformation:

$$\xi_1(\omega) = 1 + \frac{2}{\pi} P \int \frac{\xi_2(\omega')\omega'}{(\omega')^2 - \omega^2} \, \mathrm{d}\omega$$

In Figs. 8(b) and 9(b) we illustrate our calculated real part of the dielectric function. We have calculated the static dielectric constant $\xi_1(0)$ in the limit of zero frequency for MgS, MgSe and MgTe in zinc blende and rocksalt structure; the values estimated are given in Table 5.

3.4.2. Absorption coefficient

For the calculation of the absorption coefficient we used the following formula:

$$a^{\lambda}(\omega) = \frac{1}{\Omega} \sum \sum |\langle \psi_i | r^{\lambda} | \psi_{nk} \rangle|^2 \partial(E_n(k) - E_i - \hbar\omega)$$

where λ denotes the ordinary or extraordinary polarisation.

The curve of spectral dependence of the coefficient as a function of the wave length in Figs. 8(c) and 9(c) has several absorption regions. The first one is in MgS and MgSe curve; we can see that this compound can absorb all frequency regions that existed in ultraviolet light, whereas in MgTe curve we remark the same absorption but it has few characteristics that can exist in visible light.

Table 5
Values of the real part $\xi_1(0)$ of the static dielectric constant for MgS, MgSe and MgTe using the LDA calculation

Compound	$\xi_1(0)$	
	Zinc blende	Rocksalt
MgS	4.506	5.811
MgSe	5.167	6.852
MgTe	6.091	9.266

4. Conclusion

We have verified through calculations on Magnesium-based semiconducting systems that the equilibrium lattice constants, bulk modulo and their first derivatives are described equally by LDA. We have studied two different phases: zinc blende and rocksalt.

Our results show that at zero pressure, the rocksalt phase is found to be most stable for MgS, MgSe and MgTe. The preference of the rocksalt phase in Mg-based compound over the zinc blende is consistent with picture that materials with higher f_i values favour more ionic structure like rocksalt. Our results show that MgS, MgSe and MgTe have direct gap (Γ, Γ) in zinc blende structure and indirect gap (Γ, X) in rocksalt structure. The LDA curves of the DOS present the same aspect in zinc blende and rocksalt structure for MgS, MgSe and MgTe compounds.

The reported calculations provide new structural and electronic results from first principle for these compounds. The results reveal the fundamental importance of the chemical bonding nature and ionicity in determining the properties of these compounds. Our results indicate that MgS, MgSe and MgTe exhibit large ionicity character. We have also calculated the dielectric function of our compounds (MgS, MgSe and MgTe) in zinc blende and rocksalt structure using FPLAPW method and we also predicted the absorption coefficient.

Our first principles calculations in these kinds of materials will certainly be very useful for the interpretation of future experiments.

References

[1] Y. Morinaga, H. Okuyama, K. Akimoto, Jpn. J. Appl. Phys. 32 (1993) 678.
[2] P. Blaha, K. Schwartz, J. Luitz, WIEN'97: a full potential linearized augmented plane wave for calculating crystal properties, Technical University of Vienna, Vienna, 1997 (this is an improved and updated Unix version of the original copyrighted WIEN code, which was published in P. Blaha, K. Schwartz, P.I. Sorantin, S.B. Trickey (Eds.), Comput. Phys. Commun. 59 (1990) 399).
[3] W. Kohn, L.J. Sham, Phys. Rev. A 1133 (1965) 140.
[4] P. Hohenberg, W. Kohn, Phys. Rev. B 864 (1964) 136.
[5] D.M. Ceperley, B.J. Alder, Phys. Rev. Lett. 45 (1980) 566.
[6] J.P. Perdew, A. Zunger, Phys. Rev. B 23 (1981) 5048.
[7] H.J. Monkhost, Pack, Phys. Rev. B 13 (1976) 5188.
[8] F.D. Murnaghan, Deformation of an Elastic Solid, Wiley, New York, 1951 (Chapter 4).
[9] S. Lee, K.J. Chang, Phys. Rev. B 52 (1995) 1918.
[10] D. Wolverson, et al., Phys. Rev. B 64 (2001) 113203.
[11] B. Freytag, J. Phys. Condens. Matter 6 (1994) 9875.

[12] J.C. Phyllips, Bonds and Bands in Semiconductors, Academic Press, New York, 1973.
[13] A. Garcia, M.L. Cohen, Phys. Rev. B 47 (1993) 42155.
[14] M. Alouani, J.M. Wills, Phys. Rev. B 54 (1996) 2480.
[15] J.P. Hughes, J.E. Sipe, Phys. Rev. B 53 (1996) 10751.
[16] C.Y. Yeh, Z.W. Lu, S. Froyen, A. Zunger, Phys. Rev. B 46 (1992) 10086.
[17] C. Bradford, et al., Phys. Rev. B 64 (2001) 195309.
[18] A. Waag, et al., J. Cryst. Growth 131 (1993) 607.
[19] R.W.G. Wyckoff, Crystal Structures, Wiley, New York, 1963.
[20] A. Fleszar, Phys. Rev. B 64 (2001) 245204.
[21] M. Cardona, G. Harbeke, Phys. Rev. A 137 (1965) 1467;
M. Balkanski, Y. Petroff, in: Proceedings of the Seventh International Conference on the Physics of Semiconductors, Dunord, Paris, 1964;
J.W. Baars, in: D.G. Thomas, W.A. Benjamin (Eds.), Proceedings of the II–VI International Conferences on Semiconducting Compounds, New York, 1967.;
C.J. Visely, D.W. Langer, Phys. Rev. B 4 (1971) 451.
[22] H. Okuyama, et al., J. Cryst. Growth 117 (1992) 139.
[23] S.G. Parker, et al., J. Electrochem. Soc. 118 (1971) 979.
[24] T.Y. Chung, et al., Semicond. Sci. Technol. 12 (1997) 701.
[25] J.M. Hartmann, J. Appl. Phys. 80 (11) (1996) 6257.